Characterization and Modelling of Triply Periodic Minimum Surface (TPMS) Lattice Structures for Energy Absorption in Automotive Applications

N. D. Cresswell, A. A. H. Ameri, J. Wang, H. Wang, P. Hazell, and J. P. Escobedo-Diaz

Abstract The performance of triply periodic minimum surface (TPMS) lattice structures was evaluated for use as energy absorbers in automobile crash structures. Schoen's Gyroid TPMS lattice structures were manufactured from colorFabb carbon fibre reinforced nylon (PA-CF) filament using fusion deposition modelling (FDM) 3D printing. Compressive and energy absorption performance was quantified experimentally using quasi-static compression testing. Test samples were replicated at different gyroid cell size and continuous surface thickness combinations. Results were compared to published data from other lattice structures to assess relative performance, and analysed to develop a recommended gyroid TPMS geometry. It was determined that varying either the continuous surface thickness, or unit cell size influenced the performance of the structure. A gyroid TPMS structure with a cell size of 10 mm, and a continuous surface thickness of 2 mm was found to perform the best, achieving an impressively high specific energy absorption capacity of 13.06 J/g (± 0.15), significantly outperforming both 3D truss and traditional 2D lattice structures for use in the automotive industry.

Keywords Characterization · Modeling and simulation · Additive manufacturing

N. D. Cresswell · A. A. H. Ameri · J. Wang · H. Wang · P. Hazell · J. P. Escobedo-Diaz (✉)
University of New South Wales at the Australian Defence Force Academy, Canberra, ACT 2600, Australia
e-mail: j.escobedo-diaz@unsw.edu.au

Z. Peng et al. (eds.), *Characterization of Minerals, Metals, and Materials 2024*, The Minerals, Metals & Materials Series, https://doi.org/10.1007/978-3-031-50304-7_28

Introduction

The primary objective of a crash structure in an automobile is to provide a crumple zone to absorb kinetic energy and lower the acceleration pulse during an accident. Crash structures aim to control the paths of load transformation and energy dissipation throughout the vehicle. Optimising the stiffness and compressive characteristics of structures subject to impact is essential to increasing the survivability of passengers in the event of a collision [1].

Recent studies have investigated the performance potential of 3D truss lattice structures as energy absorbers in automobile crash structures. Niutta et al. [2] used numerical and experimental methods to investigate the performance potential of a bumper structure composed of 3D truss lattice structures of varying thickness manufactured by fused deposition modelling (FDM) 3D printing using carbon fibre reinforced nylon filament (PA-CF). It was determined that the 3D truss lattice structure performed better than an equivalent steel structure—it weighed 25% less than steel, yet it reduced intrusion by 7%.

It has also been determined that TPMS structures perform significantly better in compression and energy absorption metrics than 3D truss lattice structures, and traditional 2D lattice structures such as honeycomb [3–5]. TMPS structures are a class of lattice which have mathematically defined surfaces inspired by structures found in nature. The surfaces repeat periodically in three-dimensional (3D) cells. Advances in modelling and additive manufacturing techniques in recent years have enabled TPMS structures to be manufactured. The excellent energy absorption characteristics of TPMS structures present an opportunity for further application. There is a need to quantify the behaviour of different TPMS structures and to better understand how specific geometries effect their performance. TPMS cell size and surface thickness are two such characteristics which could be optimised. Automotive applications of TPMS structures have been identified as having high potential and further research and development is needed to quantify the performance and optimise the design of such structures [6]. Schoen's Gyroid TPMS geometries have been investigated in recent literature, and determined to perform extremely well in compressive and energy absorption experiments when manufactured using common additive manufacturing (AM) techniques such as fusion deposition modelling (FDM) and selective laser melting (SLM) 3D printing methods [4, 5].

The aim of this study is to investigate and analyse the applicability and performance potential of triply periodic minimum surface (TPMS) structures as energy absorbers in automobile crash structures. Gyroid TPMS structures were manufactured from carbon fibre reinforced nylon, samples varied in unit cell size, and in the thickness of the continuous surface of the structure. The energy absorption potential of these various sample geometries was characterised using quasi-static compression testing methods, and their relative performance was evaluated for application in automobile crash structures.

Methods

When determining the most suitable experimental procedure, the ISO 844:2021 and ATSM D1621-16 standards were consulted [7, 8]. For this study a sample size of 50 × 50 × 50 mm was used which is consistent with Miralbes et al. [9] and is a suitable choice when accounting for test equipment requirements, sample variability, ability to up-scale results, manufacturing time, and resources. Gyroid TPMS samples had unit cell sizes (Factor C) of 10 mm or 16.67 mm, each cell size was manufactured at a continuous surface thickness (Factor T) of 1, 2 or 3 mm These values were chosen to ensure that samples had sufficiently large internal voids to enable analysis of how the structure behaved before densification. Geometry combinations were compared as a 2 by 3 factorial. In quasi-static testing, 3 replicates of each unique geometry (treatment) were tested. Replicate numbers ensured that treatment effects were not obscured by experimental variability.

Samples were manufactured using a Prusa Bear MK3S + FDM 3D printer, from 1.75 mm diameter colorFabb PA-CF filament. It was fitted with a 0.4 mm diamond-coated hardened steel nozzle, and was used in conjunction with a EIBOS 3D Cyclopes filament dryer. This ensured that the filament did not absorb moisture during the manufacturing process, which can lead to printing defects [10]. To minimise dimensional inaccuracy and maximise consistency between samples, the x, y, and z axes of the machine were calibrated prior to manufacturing. The samples were 3D modelled, meshed (0.01 mm tolerance), and exported to PrusaSlicr 2.6.0 using the nTopology 3D generative design software package (nTop). PrusaSlicr 2.6.0 was used to slice the imported mesh and convert it to a .gcode file that the 3D printer could interpret. All samples were printed using the same settings within PrusaSlicr. The nozzle and print bed temperatures were set to 275 °C and 60 °C respectively. These values were chosen as they produced the most consistent layer adhesion, and minimised defects and other undesirable artifacts common with nylon-based filaments such as stringing or warping.

Quasi-static compression testing was conducted using a Shimadzu 100 kN universal testing machine. For these tests, samples were compressed at a speed of 0.05 mm/s until the force threshold of 80 kN was reached, or the sample had significantly surpassed its densification point. Results were recorded using the TRAPEZIUM X software package and analysed using MATLAB. High resolution video of each test was recorded using a Shimadzu TRViewX, and Canon EOS DSLR camera. Table 1 shows the outputs that were calculated from the measured data. Before testing, each sample was weighed (± 0.005 g), and its height, width, and depth were measured and recorded (± 0.005 mm). Table 1 includes the most important material parameters typically considered when determining the crashworthiness of a structure, to provide a clear understanding of the compressive behaviour of a sample [2, 4].

Table 1 Parameters calculated from quasi-static testing

Name (Abbreviation)	Units	Description
Peak Crushing Force (*PCF*)	N	The peak force experienced by the sample during compression, before the plateau region
Total Energy Absorption (*EA*)	J	The area under the force–displacement curve
Specific Energy Absorption (*SEA*)	J/g	The ratio of *EA* divided by the mass of the sample
Mean Crushing Force (*MCF*)	N	The mean force of the plateau (plastic deformation) region on the force–displacement curve
Crush Force Efficiency (*CFE*)	%	The ratio between the MCF and PCF. Higher efficiency translates to an impact response that is closer to optimal energy absorption

Table 2 Key for shorthand sample identification code

Level	1	2	3
Factor C: Cell size (mm)	16.67	10.00	–
Factor T: Surface thickness (mm)	1	2	3

Sample geometries will be represented by abbreviation in the form C*x*T*y*-*n*, using treatment factors C and T (Table 2). For example, the 2nd replicate of a sample that has a cell size of 16.67 mm, and a surface thickness of 3 mm will be represented by the code C1T3-2. Table 2 shows the shorthand key.

Results and Discussion

In this section, performance of gyroid TPMS structures in energy absorption will be discussed along with the visual failure mechanisms seen during testing. The experimental results from quasi-static testing are shown in Fig. 1. Table 3 displays the mean characterised energy absorption performance of the manufactured PA-CF gyroid TPMS structures.

An analysis of variance (ANOVA) was conducted to determine the influence of cell size (Factor C) and surface thickness (Factor T) treatments on the specific energy absorption (SEA) of the samples tested, and their interactions. The *p*-value shows if a treatment is statistically significant, a smaller value indicating that the treatment had a more significant effect ($p < 0.001$ is highly significant). Table 4 summarises the results of the ANOVA analysis.

As can be seen, the *p*-values for both cell size and surface thickness (Factor C and T) are very close to zero and therefore each treatment made a highly significant impact on the specific energy absorption capacity of the structure. In Table 4, *df* refers to degrees of freedom, *SS* to the sum of squares, and *MS* to the mean squared.

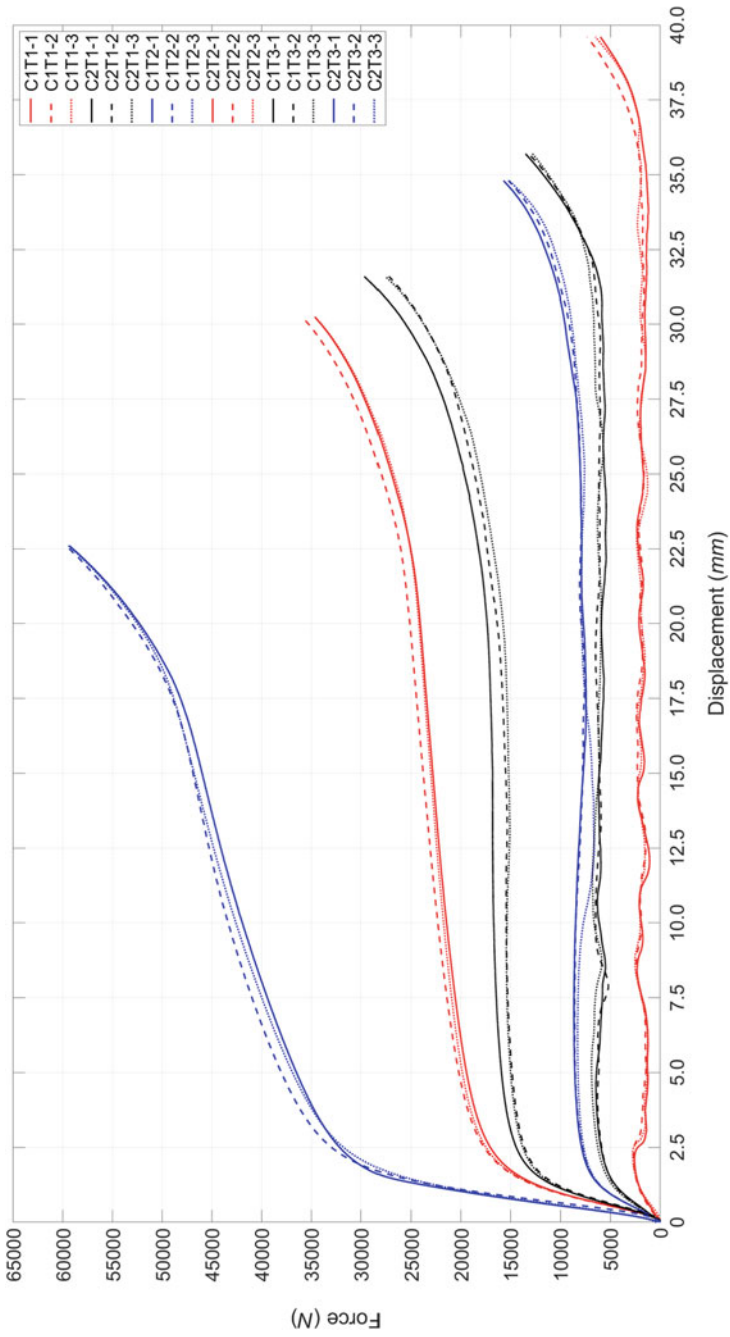

Fig. 1 Quasi-static force versus displacement curves of all treatments

Table 3 Parameters derived from quasi-static testing of gyroid TPMS structures

	Mean				
Treatment	PCF (N)	EA (J)	SEA (J/g)	MCF (N)	CFE (%)
C1T1	2673	79	5.11	2214	82.7
Std. Error	54.6	3.2	0.19	120.4	3.1
C2T1	6542	226	8.73	6368	97.3
Std. Error	179.6	4.2	0.13	200.9	1.1
C1T2	8509	288	9.16	8280	97.3
Std. Error	110.7	5.2	0.14	113.9	0.1
C2T2	20,563	698	13.06	> PCF	> 100
Std. Error	234.6	8.5	0.15	–	–
C1T3	15,856	531	11.18	≥ PCF	≥ 100
Std. Error	408.3	13.5	0.27	–	–
C2T3	36,420	951	11.70	> PCF	> 100
Std. Error	452.9	5.8	0.0	–	–

Table 4 ANOVA statistical analysis of SEA

Factors	*df*	*SS*	*MS*	*p*-value
C (Cell size)	1	32.34	32.34	0.000
T (Thickness)	2	76.10	38.05	0.000
Interaction between A and B	2	10.59	5.30	0.000
Error	12	1.00	0.08	
Total	17	120.03		

There are clear differences in performance between each treatment where only one factor varied, and the interaction between treatments was also highly significant. This is reflected in Fig. 1, and the characterised performance measures in Table 3.

Figure 1 shows that the three treatments C2T2, C1T3, and C2T3 exhibited foam-like behaviour when compressed [2, 11]. This is reflected by the MCF being greater than the PCF, resulting in a CFE exceeding 100% efficiency. All C1T3 replicates were between 100 and 102% efficiency. However, for the purpose of this study the MCF and CFE metrics will not be used as a performance comparison for the C2T2, C1T3, or C2T3 treatments.

It was observed in testing, and reflected in Fig. 1 that both T1 treatment sample sets (1 mm surface thickness) exhibited sequential layer collapse throughout compression, beginning with the top cell layer. This can be seen in the wave-like pulses in Fig. 1 for the relevant samples, caused by extensive buckling and associated print layer delamination. T1 treatment samples also experienced the least initial isotropic deformation, correlating with having the smallest elastic deformation region, shown by the small initial peak in Fig. 1. C1T2 samples exhibited similar behaviour, but to a

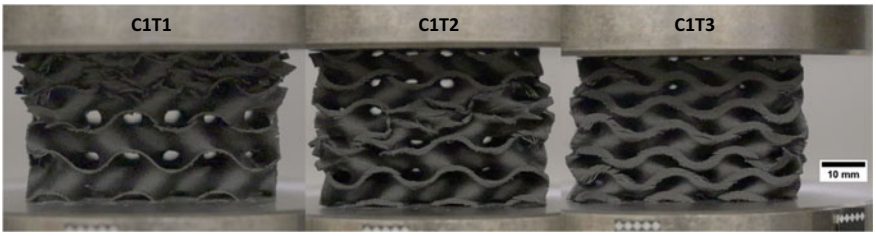

Fig. 2 C1T1-3, C1T2-3, and C1T3-3 samples under quasistatic compression

lesser extent as there was more initial isotropic deformation which instead progressed to diagonal shear failure through the central cell layers of the sample. This behaviour can be seen in Fig. 2 which shows a side-by-side comparison of all C1 treatments under compression. Shear failure behaviour across the width of the sample was not observed in any other treatments.

All other T2 and T3 treatment samples experienced isotropic deformation to collapse, and densification. It could be seen that this also correlated to an increased elastic deformation region, and a foam-like plastic deformation region. It was also observed that T2 and T3 treatments were much less prone to failure due to buckling, instead bulging outwards throughout compression, without ejecting fragments, unlike T1 treatments.

Initial print layer delamination began on the outer-most edges of the sample for all treatments. It should also be noted that only the outer face of the structure was able to be observed during testing, therefore making it impossible to observe exactly how the internal cells failed.

C1T1 samples had the lowest PCF, corresponding with a relatively small elastic deformation region. Print layer delamination was seen to begin at very small displacements, starting around the midpoint of the unit cell at the edges of the sample. The samples experienced sequential layer collapse, originating from brittle buckling failures in the top-most cell layer (Fig. 2), and localised shear failures through the midpoints of the outer edges of the continuous surface. Minor fragmentation was observed during collapse, once all layers were compressed to complete failure, the sample began to densify. This was consistent across all replicates. It can be seen in Table 3 that this treatment had the worst characterised performance, despite still having a relatively high SEA and CFE when compared to other high performing 3D lattice structures [2]. Buckling, and sequential layer collapse during quasistatic compression has also been reported for gyroid TPMS samples with a similar Factor C to Factor T ratio manufactured using a selective laser melting (SLM) printer from Ti–6Al–4V [12].

C2T1 samples performed significantly better than C1T1 treatments, despite exhibiting the same failure mechanisms. Samples with this treatment had noticeably more initial isotropic deformation, which corresponded with a PCF of ~ 2.5 times higher than C1T1 samples. Therefore, cell size has a large impact on the

energy absorption capability of gyroid TPMS structures. Initial print layer delamination was again seen at the edges of the structure at relatively low displacements, which progressed into buckling failure induced by localised shear failures in the outer continuous surface. This was followed by sequential cell layer collapse from top to bottom as the displacement increased. Due to the smaller cells, this behaviour was not as pronounced throughout the plastic region in Fig. 1 as it was for C1T1 samples. Once collapsed, the structure began to densify, which was consistent across all treatments.

Samples with the C1T2 treatment performed significantly better than C1T1 samples, outperforming C2T1 in all characterised performance measures. Samples experienced isotropic deformation until displacement exceeded ~ 8 mm. As discussed, C1T2 samples experienced diagonal shear failure through central cell layers. This was initiated by print layer delamination throughout the peaks and valleys of the outer continuous surface. This is likely due to these locations having the weakest print layer adhesion as there is no structure above or below to provide support during the printing process. Internal features, away from cell edges are self-supported and where higher stress concentrations are located in gyroid TPMS structures [4, 12].

C2T2 samples had the highest SEA of all measured treatments, significantly outperforming all equivalent PA-CF 3D truss lattice structure geometries explored by Niutta et al. [2]. Notably, they also outperformed C1T3 samples in all characterised performance measures. This suggests that increased cell count, and therefore higher areal density has a large effect on the energy absorption capacity of gyroid TPMS structures. As with other T2 and T3 treatments, the samples were seen to bulge outwards during isotropic compression (Fig. 2), and did not eject any fragments. The highest performing treatments C2T2, C1T3, and C2T3 consisted of the highest areal density, and all exhibited foam-like compression behaviour as shown in Fig. 1. This is when the CFE exceeds 100%, caused by the average force throughout plastic deformation region surpassing the PCF [11].

Figure 3 shows how the sample C2T3-2 behaved throughout quasi-static compression. At a displacement of ~ 10 mm, the cell layers can be seen compressing as the distance from peak to peak of the outer surface decreases, which is most apparent through the central cell layers. Print layer delamination through the outer surface is also apparent, concentrated around the outermost edges of the sample as they begin to bulge. At ~ 25 mm displacement, the sample has completely collapsed and is approaching maximum densification. This behaviour was consistent across all C2T3 replicates. C1T3 treatments followed an equivalent failure mechanism, however they exhibited more pronounced and widespread print layer delamination throughout the outer continuous surface.

Figure 4 shows a side-by-side comparison of C1T3 samples before and after quasi-static compression testing. The microscopic image is taken from above the sample, and focuses on the ‘trough’ between two outer continuous surface waves. The dashed arrows highlight the ‘valleys’ that contour downwards from the ‘trough’ on the left side of both images, whereas the solid arrows show the direction of the contour that rises up to the outer surface edges. It can be seen in Fig. 4 that the printed layers have significantly bulged throughout compression. This is notable as

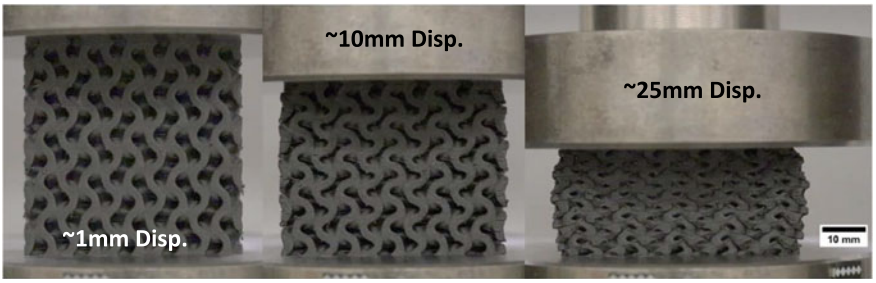

Fig. 3 C2T3-2 under quasistatic compression at varying displacements

it helps to understand how the colorFabb PA-CF polymer composite gyroid TPMS structure behaved, particularly for samples with greater surface thickness, such as T2 and T3 treatments. It also showed that given enough surrounding material, the printed layers deformed and bulged first, before any delamination occurred. It is this bulging behaviour that may promote isotropic deformation in the aforementioned treatments, as the continuous surface is predominately compressing not through print layer delamination and buckling failure, but instead by compacting the print layers which in turn causes the cell layers to deform and collapse. This also helps to explain why C2 treatments saw increased bulging during compression, as there were less internal voids to fill due to the reduced cell size, forcing material to the outer extremities of the sample.

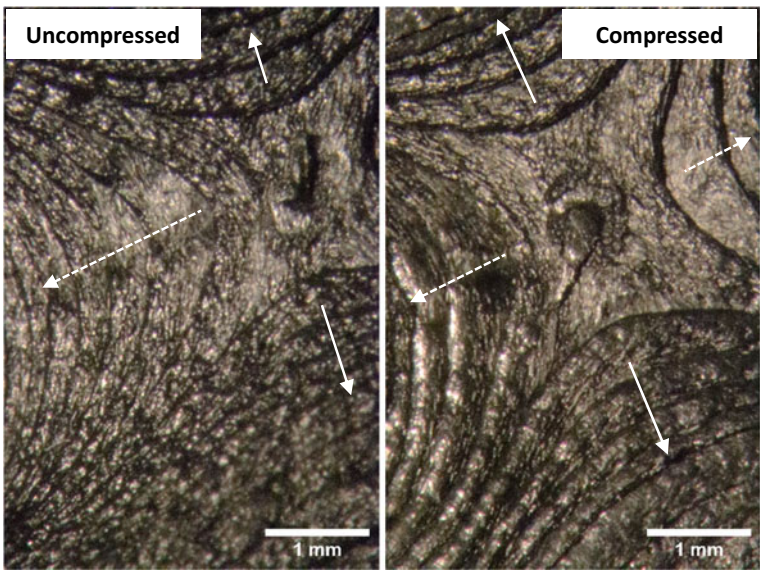

Fig. 4 Microscopic images of an uncompressed, and compressed C1T3 sample

Gyroid TPMS lattice structures manufactured from PA-CF carbon fibre reinforced nylon, with 10 mm cell size and 2 mm surface thickness (C2T2), yielded the best specific energy absorption (SEA) from the different geometries tested. The PA-CF 3D truss lattice structures explored by Niutta et al. [2] achieved a maximum SEA of 7.53 J/g, which significantly outperforms traditional 2D lattice structures. Yin et al. [4] reported an SEA value of 20.04 J/g for gyroid TPMS structures manufactured using a SLM 3D printer from 316 L stainless steel. The C2T2 treatment explored in the current study achieved an impressively high SEA value of 13.06 J/g ($\pm$ 0.15), outperforming PA-CF 3D truss structures, and approaching SEA values achieved by 316 L stainless steel gyroid samples.

The C2T2, and both T3 geometries were found to compress isotopically, and responded to quasi-static compression similarly to a foam. This characteristic is very desirable as it means that the structure exhibits behaviour similar to a spring, in which it requires an increasingly high amount of force to compress the structure throughout its plastic deformation region.

Gyroid TPMS lattice structures have considerable potential for application as energy absorbing structures in the automotive industry. For an automobile crash structure to function successfully, it must be able to provide a crumple zone to absorb kinetic energy and lower the acceleration pulse during an accident. It must also be compact, lightweight, and cost effective—to not adversely impact vehicle performance or affordability. To accommodate a wide range of collision scenarios, a crash structure should have zones designed to deal with different magnitudes of impact energy. It was seen in this study that varying the cell size, and/or continuous surface thickness, of PA-CF gyroid TPMS structures yielded highly efficient, lightweight energy absorbers capable of performing extremely well in a variety of impact scenarios. The self-supporting nature of the structure further enhances its applicability, as manufacturing difficulty and variability is reduced when using inexpensive FDM 3D printing methods.

Conclusion

Schoen's Gyroid TPMS lattice structures manufactured from carbon fibre reinforced nylon (PA-CF) were shown to have large specific energy absorption (SEA) capacity. Varying either the continuous surface thickness, or unit cell size, significantly influenced the performance of the structure. The interaction between surface thickness and cell size was also highly significant in affecting SEA. A gyroid TPMS structure with a cell size of 10 mm, and a continuous surface thickness of 2 mm was found to perform the best, achieving a SEA value of 13.06 J/g. This exceeds reported specific energy absorption capacity of both traditional 2D lattice structures and 3D truss geometries made from PA-CF and approaches that are of SLM printed 316 L stainless steel.

Some of the gyroid TPMS lattice geometries were shown to compress isotopically, and respond to quasi-static compression similarly to a foam, so that as the structure is compressed, more energy is required to compress it further. PA-CF was well suited to the application, yielding repeatable, high strength, yet lightweight samples that were easy to manufacture. The observed compressive behaviour means that gyroid TPMS lattice structures have considerable potential for application as energy absorbers in automobile crash structures.

Acknowledgements N. Cresswell would like to acknowledge the Australian Government Department of Defence for providing the Defence Civilian Undergraduate Scholarship program which supports his studies.

References

1. Vangi D (2020) Structural behavior of the vehicle during the impact. In: Vehicle collision dynamics—analysis and reconstruction. Butterworth-Heinemann, p 1–27
2. Niutta CB, Ciardiello R, Tridello A (2022) Experimental and numerical investigation of a lattice structure for energy absorption: application to the design of an automotive crash absorber. Polymers 14(6):11160. https://doi.org/10.3390/polym14061116
3. Sokollu B, Gülcan O, Konukseven EI (2022) Mechanical properties comparison of strut-based and triply periodic minimal surface lattice structures produced by electron beam melting. Addit Manuf 60:103199. https://doi.org/10.1016/j.addma.2022.103199
4. Yin H, Liu Z, Dai J, Wen G, Zhang C (2020) Crushing behavior and optimization of sheet-based 3D periodic cellular structures. Compos Part B 182:107565. https://doi.org/10.1016/j.compositesb.2019.107565
5. Peng C (2022) Novel lattice structures based on triply periodic minimal surfaces. Royal Melbourne Institute of Technology—Research Repository. https://researchrepository.rmit.edu.au/esploro/outputs/doctoral/Novel-lattice-structures-based-on-triply/9922198113301341. Accessed 5 Sept 2023
6. Yin H, Zhang W, Zhu L, Meng F, Liu J, Wen G (2023) Review on lattice structures for energy absorption properties. Compos Struct 304(1):116397. https://doi.org/10.1016/j.compstruct.2022.116397
7. ISO 844:2021: Rigid cellular plastics—determination of compression properties (2021). https://www.iso.org/standard/73560.html. Accessed 20 Aug 2023
8. ASTM D1621-16: Standard test method for compressive properties of rigid cellular plastics (2016). https://www.astm.org/d1621-16.html. Accessed 21 Aug 2023
9. Miralbes R, Ranz D, Pascual FJ, Zouzias D, Maza M (2020) Characterization of additively manufactured triply periodic minimal surface structures under compressive loading. Mech Adv Mater Struct 29(13):1841–1855. https://doi.org/10.1080/15376494.2020.1842948
10. Banjo AD, Agrawal V, Auad ML, Celestine A-DN (2022) Moisture-induced changes in the mechanical behavior of 3D printed polymers. Compos Part C 7:100243. https://doi.org/10.1016/j.jcomc.2022.100243
11. Xing Y, Sun D, Zhang M, Shu G (2023) Crushing responses of expanded polypropylene foam. Polymers 15(9):2059. https://doi.org/10.3390/polym15092059
12. Yang E, Leary M, Lozanovski B, Downing D, Mazur M, Sarker A, Khorasani AM, Jones A, Maconachie T, Bateman S, Easton M, Qian M, Choong P, Brandt M (2019) Effect of geometry on the mechanical properties of Ti-6Al-4V gyroid structures fabricated via SLM: a numerical study. Mater Des 184:108165. https://doi.org/10.1016/j.matdes.2019.108165